physica status solidi

pss

www.pss-journals.com

reprint

WILEY-VCH

Phys. Status Solidi A **212,** No. 4, 826–830 (2015) / **DOI** 10.1002/pssa.201431605

physica status solidi a
www.pss-a.com
applications and materials science

ZnO TFTs prepared by chemical bath deposition technique with high-*k* La_2O_3 gate dielectric annealed in ambient atmosphere

Paragjyoti Gogoi*[,1], Rajib Saikia[1], Dipok Saikia[1], Ronen Prakash Dutta[2], and Sanjib Changmai[1]

[1] Department of Physics, Thin Film Laboratory, Sibsagar College, Joysagar 785665, Assam, India
[2] Department of Electronics, Sibsagar College, Joysagar 785665, Assam, India

Received 25 August 2014, revised 25 November 2014, accepted 8 December 2014
Published online 30 January 2015

Keywords CBD technique, La_2O_3, low threshold voltage, mobility, ZnO TFT

* Corresponding author: e-mail paragjyoti_g@rediffmail.com, Phone: +91 9854809816, Fax: 03772-270578

In this paper, the electrical properties of top-gated thin-film transistors with low-cost chemical bath deposition (CBD) of ZnO as active material and a high-*k* rare-earth oxide La_2O_3 as gate dielectric have been reported. The source-drain and gate electrodes and dielectric layers are fabricated by thermal evaporation techniques in high vacuum of the order of 10^{-6} Torr in a coplanar electrode structure. The channel length of the TFT is of 50 μm. The fabricated TFTs are annealed at 500 °C in air. The TFTs exhibit a field effect mobility 0.58 ($cm^2 V^{-1} s^{-1}$). Use of a high dielectric constant (high-*k*) gate insulator reduces the threshold voltage and subthreshold swing of the TFTs. The TFTs exhibit a low threshold voltage of 4 V. The calculated values of gain–bandwidth product and subthreshold swing are also evaluated and presented. The ON/OFF ratio of the TFT is found to be 10^6.

1 Introduction During the last decades the studies of ZnO thin films have received much attention due to their potential applications as gas sensors, transparent conducting electrodes, solar cell windows, etc. Due to the wide bandgap (3.37 eV) and high excitation binding energy (60 meV) ZnO is a strong candidate for light-emitting diodes and other photovoltaic devices [1]. ZnO is also widely used in high-temperature electronics devices that are reliable for space and other high environments. Nowadays, ZnO is widely used as the active material in TFTs because of its transparency and high field effect mobility, high mechanical, thermal, and chemical stability [2–4]. Many investigators have reported that silicon-based TFTs have limited applications due to their low field effect mobility, light sensitivity, and small drain current. Also, ZnO thin films required a relatively low deposition temperature to grown as crystallite material on various substrates such as silicon or glasses than that of silicon [5]. Therefore, ZnO-based TFTs have received significant attention in recent years as an alternative to silicon-based TFTs [6–10].

ZnO thin films have been fabricated and synthesized by variety of processes, namely thermal deposition, chemical bath deposition, metal organic chemical vapor deposition spray pyrolysis, sol gel, etc. Among the various techniques, chemical bath deposition is one of the simplest and cost-effective techniques for the deposition of semiconductors and ceramic film deposition that provides a thin film having uniform surface [11, 12]. More generally in CBD techniques, an aqueous solution made up of some mixture of precursor solution and complexing agents and the substrates for the deposition of the films are required.

The rare-earth oxide La_2O_3 exhibits very high dielectric constant (14.77) [13] and low leakage current and hence is reliable as a dielectric in microelectronics, and recently La_2O_3 is under intense investigation for replacing conventional SiO_2 [14, 15]. Due to the properties of insensitivity to impurities and being more stable owing to the absence of grain boundaries, amorphous dielectrics are suitable for gate dielectrics. Up till now many investigators have successfully used La_2O_3 as a gate insulator in TFTs [16–18].

In this paper we report the chemical bath deposition of ZnO thin films, their characterization and performance of ZnO thin film as active material in TFTs. The electrical

characteristics and the various parameters are evaluated using theoretical model and presented. The CBD method used to prepare ZnO thin film is a modification of the method used by Chatterjee et al. [19].

2 Experimental details The ZnO films are deposited by a chemical bath deposition method. First, glass slides are cleaned ultrasonically to use as substrates. For the deposition of ZnO on glass substrates, a sodium zincate (Na_2ZnO_2) bath is prepared. For the preparation of the Na_2ZnO_2 bath, first 100 ml of 0.1 M $ZnCl_2$ aqueous solution is prepared using deionized water. Then, NaOH is added into the $ZnCl_2$ solution to prepare the (Na_2ZnO_2) bath. The mixture is then stirred by a magnetic stirrer for 30 min. Initially, a white precipitate of zinc hydroxide ($Zn(OH)_2$) is formed. A clear solution is obtained after addition of 60 ml of 4 M NaOH solution into the bath. The mixer is again stirred for 30 min. In the entire process the bath temperature is maintained at 40 °C. The pH of the solution is 11. The chemical reactions are as follows:

$$ZnCl_2 + 2NaOH = Zn(OH)_2 + 2NaCl,$$

$$Zn(OH)_2 + 2NaOH = Na_2ZnO_2 + 2H_2O.$$

The ZnO thin films are deposited on the substrates by alternate dipping into the (Na_2ZnO_2) bath and then into a hot water bath. This leads to the reaction

$$Na_2ZnO_2 + H_2O = ZnO + NaOH.$$

The zinc hydroxide is formed due to hydrolysis of deposited ZnO during subsequent immersions in hot water [20]. The film thickness can be increased by increasing the immersion time in the bath. In this investigation the number of immersion is 20–25 and the immersion time is 5 s into the two baths for deposition of each ZnO films. The as-deposited films are then annealed at 500 °C for 1 h in air. The thicknesses of the films are measured using Tolanky's multiple mean interference method [21].

The TFTs are fabricated in a top-gated coplanar electrode structure. The source-drain and gate electrodes and the dielectric layer are deposited by a thermal evaporation method under high vacuum of the order of 10^{-6} Torr. The different fabrication steps of the TFTs are as follows:

(i) The ZnO thin films of 500 Å are deposited on the glass substrates by the CBD technique as mentioned above.
(ii) Al source-drain electrodes are deposited over the ZnO film maintaining a channel of length 50 μm. and channel width of 0.1 cm.
(iii) Grade purity rare-earth oxide La_2O_3 without further purification is deposited over the source–drain electrodes as gate dielectric layer of 800 Å.
(iv) Over the dielectric layer Al is deposited as a gate electrode.

A schematic diagram of the fabricated TFT is shown in Fig. 1.

3 Results and discussion The polycrystalline structure and the surface morphology of the ZnO films are investigated through an XRD spectrum (Fig. 2) and SEM analysis (Fig. 3). In Fig. 2, curves a and b show XRD spectra without annealing and with annealing at 500 °C, respectively. No distinct peaks are observed in case of ZnO films without annealing (curve a). But four distinct peaks (100), (002), (101), and (110) of ZnO are observed in the XRD spectrum in case of the annealed films at 500 °C in air, which confirms the preparation of ZnO thin films by the CBD method (curve b). The SEM micrograph shows a uniform granular structure of the ZnO films. The average size of the ZnO crystallites is calculated from the XRD pattern using the Debye–Scherer's formula (Eq. (1)) as follows and found to be 117 nm.

$$d = \frac{k\lambda}{\beta\cos\theta}, \tag{1}$$

where λ is the wavelength of X-ray radiation used, β is the angular line width at half of the maximum intensity, θ is the Bragg diffraction angle and k is a constant.

Well-modulated I_D–V_D characteristics at various gate voltages (V_G) of the fabricated TFTs with an air-annealed sample are observed, which are shown in Fig. 4. The drain current is significantly increased and shows well-saturated characteristics from 12 V gate voltage onwards and complete pinch off occurs at 2 V gate voltage. The TFTs are operated in enhancement mode. Figure 5 shows the I_D–V_D characteristics of TFTs in a sample without annealing that shows low drain current with respect to drain voltage than that of the TFTs with an air-annealed ZnO sample.

The $(I_D)^{1/2}$–V_G plots for the TFTs at constant drain voltage $V_D = 10$ V are shown in Fig. 6. In Fig. 6, curves a and b are for the TFTs with air annealing and without air annealing, respectively. From the extrapolation of the linear portion of the graph to the V_G axis of the plots, the threshold voltages (V_T) of the devices are calculated. In the saturation region $V_D = V_G$–V_T, the drain current is given by Eq. (2) [22] on the basis of which the electrical parameters are evaluated.

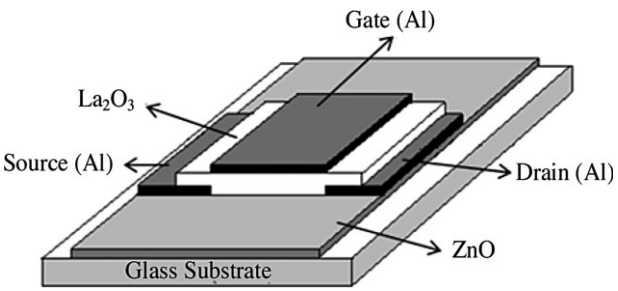

Figure 1 Schematic diagram of the coplanar electrode structure of the TFTs.

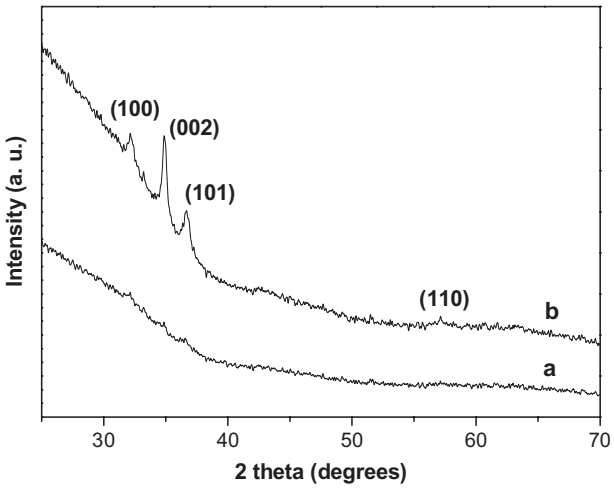

Figure 2 XRD spectrum of the ZnO thin film. Curve (a), without annealing; curve (b), annealed at 500 °C in air.

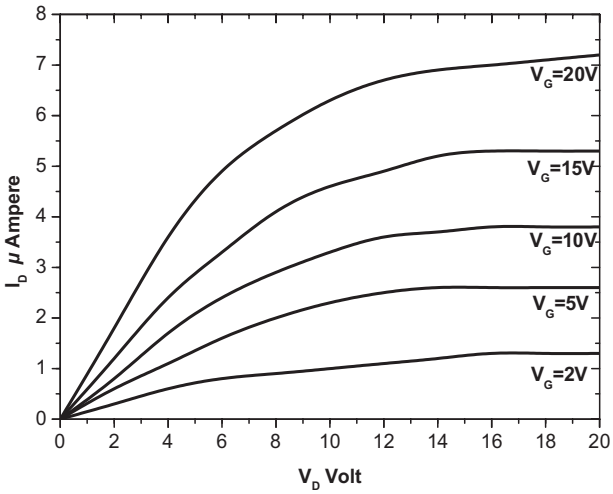

Figure 4 I_D–V_D characteristics of air annealed ZnO TFTs at constant V_G.

$$I_{Dsat} = \frac{W}{2L}\mu_{FE}C_i(V_G - V_T)^2, \tag{2}$$

where W is the channel width, L is channel length, C_i is the gate capacitance per unit area, V_T is the threshold voltage and μ_{FE} is the field-effect mobility. The field-effect mobility μ_{FE} is calculated from the slope of this plot. The gain–bandwidth product is the measure of high-frequency performance of the devices. The gain–bandwidth (G.Bw.) product of the device is evaluated from Eq. (3) [23]

$$\text{G.Bw.} = \frac{g_m}{2\pi C_i}. \tag{3}$$

The plot of log (I_D) versus V_G at a constant drain voltage ($V_D = 10$ V) is shown in Fig. 7 in which curves a and b represent the TFTs with air annealing and without air annealing, respectively. The subthreshold swing is calculated from the slope of these graphs using the relation [24]

$$s = \left(\frac{\delta(\log I_D)}{\delta V_G}\right)^{-1}. \tag{4}$$

The drain current ON–OFF ratio of the device is calculated from the relation [20]

$$\frac{I_{ON}}{I_{OFF}} = \frac{C_i\mu_{FE}(V_G - V_T)^2}{\sigma d V_D}, \tag{5}$$

where σ and d are conductivity and thickness of the semiconductor of the TFTs, respectively.

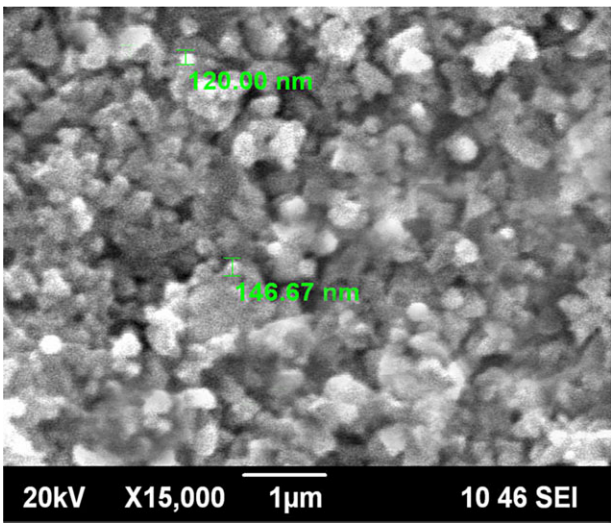

Figure 3 SEM image of the ZnO thin film.

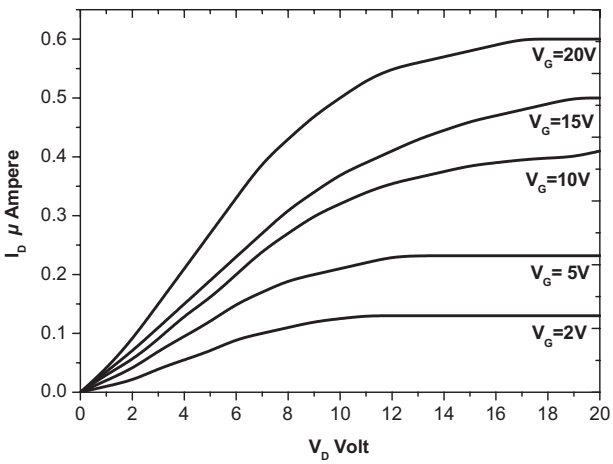

Figure 5 I_D–V_D characteristics of without annealed ZnO TFTs at constant V_G.

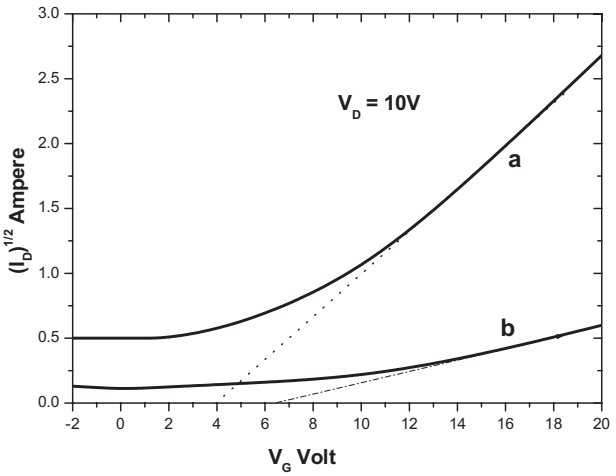

Figure 6 I_D–V_G plots for ZnO TFTs at constant drain voltage $V_D = 10$ V. Curves (a) and (b) are for TFT with air annealing and without air anneal, respectively.

The J–V characteristic of the dielectric film in Al/La_3O_3/Al configuration is shown in Fig. 8. From Fig. 8 it is seen that the dielectric film shows a very low leakage current and thereby proves the suitability for use as a dielectric layer in thin-film transistors.

The calculated values of mobility, threshold voltage, subthreshold swing, a gain–bandwidth product and drain current ON–OFF ratio of the devices are presented in Table 1 and the results are compared with the TFT with and without annealed ZnO thin films. Table 2 contains a comparison of the calculated parameters with some previous results [16, 25, 26], which shows significant improvement over that of the previous investigations. The slightly lower value of the mobility in the present investigation (0.58 cm^2/V s) than that of the previous [16] (0.77 cm^2/V s) is due to the use of a nonpatterned ZnO channel layer, whereas they have used patterned channel layer that reduces the off current. From the results mentioned in Table 2 it can be inferred that good electrical properties are exhibited by the fabricated TFT with the air-annealed sample. High values of field effect mobility and ON–OFF ratio are exhibited by the TFTs. The threshold voltage and subthreshold swing are found to be relatively low. The gain–bandwidth product of the TFTs is also high, which is due to the high field effect mobility. The high value of the mobility of the TFT is due to the fact that as the TFT is annealed in air at high temperature (500 °C), the oxygen content in the films may increase, which provides good-quality ZnO films. At high annealing temperatures passivation of the oxygen atoms into the interstitial positions of the ZnO crystals and reduction of the trapping of charges in the grain boundaries occur. This leads to the reduction of potential barrier at the grain boundaries and consequently the mobility of the carrier increases. The mobility of the devices may further be increased by annealing the devices in an oxygen atmosphere that can passivate the oxygen vacancies that create deep levels in the bandgap structure [25, 27]. No significant results are observed in case of the TFTs using ZnO films without annealing because trapping of charge carriers in the grain

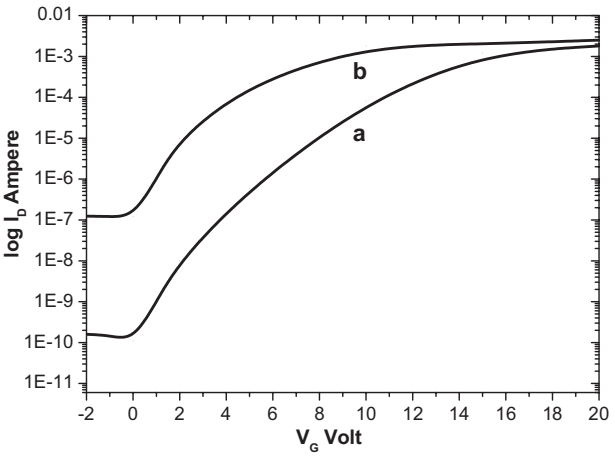

Figure 7 The plots of log (I_D)–V_G at constant drain voltage. Curves (a) and (b) are for TFT with air annealing and without air anneal, respectively.

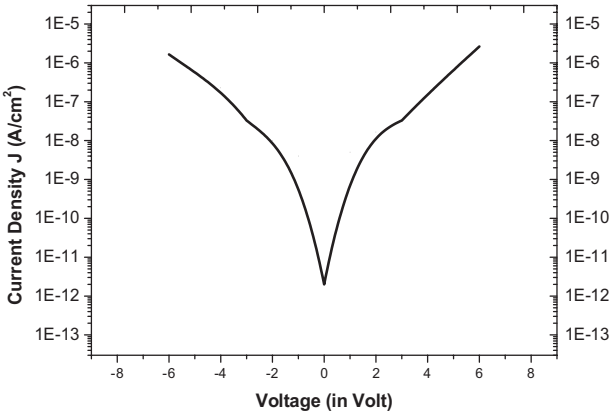

Figure 8 J–V characteristics of Al/La_2O_3/Al structure.

Table 1 Comparison of the measured values of electrical parameters of TFTs with air annealed and without annealed sample.

parameters	TFT with air annealed sample	TFT without annealed sample
mobility (μ_{FE}) (cm^2/V s)	0.58	0.024
threshold voltage (V_T) (V)	4	6.6
ON–OFF ratio	10^6	10^4
subthreshold swing (V/decade)	1	1.1
gain–bandwidth product (G.Bw.) (kHz)	0.04	0.039×10^{-3}

Table 2 Measured values of field effect mobility (μ_{FE}), threshold voltage (V_T), gain–bandwidth product (G.Bw.), drain current ON–OFF ratio, and subthreshold swing of the fabricated devices and comparison of these parameters with some previous results with different gate dielectrics and method of preparation.

parameters	present results (La_2O_3) (annealed in air)	previous results (PVP) [25] (oxygen-annealed) (CBD method)	previous results (SiO_2) [26] (sol–gel method)	previous results (La_2O_3) [16] (sputtering method)
mobility (μ_{FE}) (cm^2/V s)	0.58	0.05	0.06	0.77
threshold voltage (V_T) (V)	4	−2.1	15.6	—
ON–OFF ratio	10^6	10^2	10^5	10^5
subthreshold swing (V/decade)	1	—	—	1.2
gain–bandwidth product (G.Bw.) (kHz)	0.04	—	—	—

boundaries of the ZnO polycrystals occurs, which acts as a potential barrier and decrease the mobility as well as other electrical parameters.

4 Conclusions The ZnO-based TFTs with La_2O_3 gate dielectric were successfully fabricated by CBD and thermal evaporation techniques. The TFTs exhibited high field effect mobility, high ON–OFF ratio and low threshold voltage. From this investigation it can also be concluded that the high-*k* rare-earth oxide La_2O_3 can act as a good dielectric material in TFTs and the ZnO-La_2O_3 is a good semiconductor–insulator combination for TFTs. Furthermore, the effect of other dielectric materials and doping effects of ZnO are also under investigation for the improvement of performance of the ZnO TFTs.

Acknowledgement The authors are grateful to the University Grants Commission (UGC), New Delhi, India for providing financial assistance under Major Research Project Program.

References

[1] Y. Kim, W. Lee, D. Jung, J. Kim, S. Nam, H. Kim, and B. Parka, Appl. Phys. Lett. **96**, 171902 (2010).
[2] E. Fortunato, T. P. Barquinha, A. Pimentel, A. Goncalves, A. Marques, L. Pereira, and R. Martins, Thin Solid Films **487**, 205 (2005).
[3] D. Redinger and V. Subramanian, IEEE Trans. Electron Devices **54**, 1310 (2007).
[4] W.-Y. Chen, J. Jeng, and J. -S. Chen, ECS Solid State Lett. **1**, 5 (2012).
[5] S. Hayamizu, H. Tabata, H. Tanaka, and T. Kawai, J. Appl. Phys. **80**, 787 (1996).
[6] P. K. Nayak, J. Kim, C. Lee, and Y. Hong, Phys. Status Solidi A **207**, 1664 (2010).
[7] Y. Ohya, T. Niwa, T. Ban, and Y. Takahashi, Jpn. J. Appl. Phys. **40**, 297 (2001).
[8] P. F. Carcia, R. S. Mclean, M. H. Reilly, and G. Nunes, Appl. Phys. Lett. **82**, 1117 (2003).
[9] R. L. Hoffman, B. J. Norris, and J. F. Wager, Appl. Phys. Lett. **82**, 733 (2003).
[10] C. G. Choi, S. J. Seo, and B. S. Bae, Electrochem. Solid-State Lett. **11**, H7 (2008).
[11] J. B. Chu, S. M. Huang, D. W. D. W. Zhang,, Z. Q. Bian,, X. D. Li, and Z. Sun, Appl. Phys. **95**, 849 (2009).
[12] G. Hodes, Chemical Solution Deposition of Semiconductor Films (Marcel Dekker, New York, 2003).
[13] D. Xue, K. Betzler, and H. Hesse, J. Phys.: Condens. Matter **12**, 3113 (2000).
[14] M. Leskela, K. Kukli, and M. Ritala, J. Solid State Chem. **418**, 27 (2003).
[15] M. Leskela, K. Kukli, and M. Ritala, J. Alloys Compd. **170**, 170 (2003).
[16] Y.-K. Moon, S. Lee, J.-W. Park, D.-H. Kim, J.-H. Lee, and C.-O. Jeong, J. Korean Phys. Soc. **55**, 1906 (2009).
[17] L. X. Qian, P. T. Lai, and W. M. Tang, Appl. Phys. Lett. **104**, 123505 (2014).
[18] P. Gogoi and R. Saikia, Int. J. Electron. **99**, 869 (2012).
[19] A. P. Chatterjee, P. Mitra, and A. K. Mukhopadhyay, J. Mater. Sci. **34**, 4225 (1999).
[20] M. Ristov, G. J. Sinadinovski, I. Grozdanov, and M. Mitreski, J. Mater. Sci. **149**, 65 (1987).
[21] S. Tolansky, Surface Micro Topography (Longmans, London, 1960).
[22] B. C. Shekar, J. Lee, and S. Woo-Rhee, Korean J. Chem. Eng. **21**, 267 (2004).
[23] P. K. Weimer, Physics of Thin Films, Vol. 2, edited by B. G. Hass and R. E. Thun (Academic Press, New York, 1964), p. 147.
[24] J. H. Seo, J. Hong, S. Shin, K. S. Suh, and B. K. Ju, Semicond. Sci. Technol. **22**, 1039 (2007).
[25] P. K. Nayak, J. Jang, C. Lee, and Y. Honga., Appl. Phys. Lett. **95**, 193503 (2009).
[26] H.-C. You and Y.-H. Lin, Int. J. Electrochem. Soc. **7**, 9085 (2012).
[27] K. Vanheusden, W. L. Warren, C. H. Seager, D. R. Tallant, J. A. Voigt and B. E. Gnade, J. Appl. Phys. **79**, 7983 (1996).

